Advanced Medical Research

Global Science Publishing

Number 5 (2026), pp. 01–07

Article

Electroacupuncture at the Auricular Concha Regulates the Hippocampal SIRT1/CREB/BDNF Axis and Promotes Neurogenesis in Rats with Post-Stroke Depression

Taohong Chen [1,*], Yingsi Zhang [1], Jinqing Huang [2] and Guangjin Zhou [2]

[1] Traditional Chinese Medicine Hospital of Gaoming Foshan, Foshan 528500, China
[2] Foshan Gaoming District People's Hospital, Foshan 528500, China
* Corresponding author: 183927017@qq.com

Received: August 27, 2026; Revised: September 3, 2026; Accepted: September 10, 2026; Published: September 16, 2026

Abstract: Background and Objectives: Post-stroke depression (PSD) arises frequently after cerebral ischemia and worsens functional outcome, yet its pharmacological management remains suboptimal. Auricular-concha electroacupuncture (EA) activates afferents of the auricular branch of the vagus nerve and shows antidepressant promise; however, its effect on hippocampal neurogenesis and the underlying signaling cascade is incompletely characterized. This study examined whether EA at the auricular concha relieves depressive-like behavior and neurological deficits in PSD rats by stimulating hippocampal neurogenesis through the SIRT1/CREB/BDNF pathway. Methods: Male Sprague–Dawley rats were allocated into Control, Sham, PSD, and PSD + EA groups (n = 10). PSD was induced by permanent middle cerebral artery occlusion combined with chronic unpredictable mild stress and single housing. EA (square wave, 0.5 mA, 10/25 Hz, 30 s on/2 min off, 1 h/day, 28 days) was applied to the left auricular concha. Body weight, neurological severity (mNSS), sucrose preference, open-field, and forced-swim tests were evaluated at 24 h, 14 d, and 28 d. Neuronal morphology (HE), cell proliferation (Ki67), and the progenitor marker Nestin were assessed, and SIRT1, CREB, and BDNF expression was quantified by RT-PCR and Western blot. Results: PSD rats displayed higher mNSS, reduced body weight, lower sucrose preference and locomotion, and prolonged immobility (all $p < 0.05$ vs. Control). EA reversed each abnormality at 14 d and 28 d ($p < 0.05$ vs. PSD). Histology revealed neuronal loss and disarray in CA1, CA3, and the dentate gyrus, together with fewer Ki67-positive cells and diminished Nestin immunoreactivity; EA attenuated these changes. At the molecular level, PSD reduced SIRT1, p-CREB, and BDNF expression, which EA partially restored ($p < 0.05$ vs. PSD). Conclusion: Auricular-concha EA mitigates depressive-like and neurological deficits in PSD rats, an effect linked to enhanced hippocampal neurogenesis and re-activation of the SIRT1/CREB/BDNF cascade, supporting further translational evaluation.

Keywords: electroacupuncture; auricular concha; post-stroke depression; hippocampal neurogenesis; SIRT1; CREB; BDNF

1. Introduction

Stroke ranks among the leading causes of death and disability globally, with an estimated 17 million new cases each year [1]. Depression complicates the clinical course of stroke in a substantial proportion of survivors and is recognized as an independent contributor to poor recovery [2]. Contemporary estimates place the point prevalence of PSD between roughly 18% and 33%, with cumulative incidence approaching one-half of patients followed longitudinally [2,3]. Relative to non-depressed peers, individuals with PSD show higher long-term mortality, more severe cognitive decline, greater disability, and reduced quality of life [1]. These observations, together with the partial response rates and latency of conventional antidepressants, motivate the search for adjunctive neuromodulatory approaches.

Within the brain, the hippocampal dentate gyrus is one of the limited niches that sustain adult neurogenesis, and converging evidence positions impaired neurogenesis as a core element of depressive pathophysiology. Depressed patients exhibit smaller hippocampal volumes, and antidepressant efficacy is dependent on intact neurogenesis [4,5]. Accordingly, interventions that rescue hippocampal neuron production represent an attractive strategy for PSD. Among the trophic and transcriptional regulators of this process, brain-derived neurotrophic factor (BDNF) and the cAMP response-element binding protein (CREB) are especially well characterized: CREB phosphorylation at Ser133 drives transcription of BDNF and related genes, whereas BDNF sustains the survival, maturation, and integration of nascent neurons [6,7]. Circulating BDNF is reproducibly lower in PSD and has been proposed as a predictive biomarker [7]. Upstream of this axis, silent information regulator 1 (SIRT1), a NAD+-dependent deacetylase, governs hippocampal plasticity and neurogenesis, and its activation has been linked to antidepressant-like effects in pre-clinical models [8,9]. A SIRT1–CREB–BDNF hierarchy therefore offers a coherent framework for interpreting neurogenesis-promoting therapies.

Acupuncture is increasingly used as an adjunct for PSD, and systematic reviews support its efficacy and safety when combined with standard care [10–12]. Electroacupuncture delivers stronger and more controllable stimulation than manual needling. The auricular concha is of particular mechanistic interest because it is densely innervated by the auricular branch of the vagus nerve; stimulation of this region recruits a brainstem–hippocampal network through the nucleus tractus solitarius [13,14]. Non-invasive or transcutaneous auricular vagus nerve stimulation and auricular EA have shown antidepressant and neuroprotective effects in both clinical and experimental settings [13,15]. Consistent with this background, our group has previously reported that variable-frequency auricular vagus nerve stimulation reduces infarct volume, improves neurological recovery, and suppresses TLR4/NF-κB-driven neuroinflammation in ischemia-reperfusion rats [16].

Notwithstanding these advances, whether auricular-concha EA engages hippocampal neurogenesis, and whether this effect proceeds through the SIRT1/CREB/BDNF cascade, has not been directly established. The present study therefore evaluated, in a combined ischemia stress model of PSD, the behavioral, histological, and molecular consequences of auricular-concha EA. We hypothesized that EA would alleviate depressive-like behavior and neurological impairment while promoting hippocampal neurogenesis via SIRT1/CREB/BDNF activation.

2. Materials and Methods

2.1. Animals and Ethics

Male Sprague–Dawley rats (specific-pathogen-free; initial weight 220–250 g; age 45–55 days) were maintained under a 12/12-h light/dark cycle at 23–25 °C and 55–65% humidity with ad libitum access to chow and water. Animals acclimatized for one week prior to procedures. All experiments compiled with institutional animal ethics approval and the ARRIVE guidelines.

2.2. Grouping

Forty rats were randomized by a random-number table into four groups (n = 10 each): Control, Sham, PSD (Model), and PSD + EA. Rats that died or failed modeling were replaced to preserve group size.

2.3. PSD Model Establishment

Permanent MCAO. Body weight was maintained at 250–280 g before surgery. Under pentobarbital anesthesia, permanent middle cerebral artery occlusion was performed using the intraluminal suture method described by Longa and colleagues, and widely adopted in our prior work [16]. Neurological deficit was scored 24 h after surgery using the modified Neurological Severity Score (mNSS); animals that died, became infected, or failed scoring criteria were excluded and replenished.

Chronic stress and isolation. Surviving MCAO rats were subjected to chronic unpredictable mild stress (CUMS) combined with single housing for 21 days. Daily, one long-duration and one short-duration stressor were applied from the following repertoire, never simultaneously: food and water deprivation (20 h); water deprivation (18 h); 45° cage tilt (17 h); continuous illumination (36 h); wet bedding (21 h); 4 °C swim (5 min); spatial restraint (2 h); tail clamp (1 min); noxious noise (10 min); and horizontal shaking at 1 Hz (5 min).

2.4. Electroacupuncture

Following a previously optimized protocol [16], a 0.16 mm × 20 mm needle was inserted 1–1.5 mm subcutaneously into the left auricular concha and connected to a pulsed stimulator (square wave, 0.5 mA, 0.5 ms,

alternating 10/25 Hz, 30 s on/2 min off). Stimulation lasted 1 h daily for 28 consecutive days. Control and Sham rats received matched handling only.

2.5. Behavioral and Neurological Assessment

Evaluations were performed at 24 h, 14 d, and 28 d. Body weight was recorded electronically. Neurological impairment was scored with mNSS (0–18). Sucrose preference was measured by presenting 1% sucrose and water bottles for 1 h after habituation and deprivation, calculated as sucrose intake divided by total fluid intake. Locomotor and rearing activity were quantified in an open field over 5 min, and immobility time was recorded over 5 min in the forced-swim test (15 cm water, 25 °C).

2.6. Histology and Immunofluorescence

Deeply anesthetized rats were transcardially perfused with phosphate-buffered saline followed by 4% paraformaldehyde. Brains were post-fixed, and paraffin sections of the hippocampus were prepared. Hematoxylin–eosin (HE) staining assessed neuronal morphology in CA1, CA3, and the dentate gyrus (DG). Immunohistochemistry for Nestin (1:100) was quantified as mean optical density across five high-power fields per section. Immunofluorescence for Ki67 (1:100) and Nestin was performed with DAPI nuclear counterstain; positive cells were counted in three sections and three fields per section per animal.

2.7. RT-PCR and Western Blot

Hippocampi were snap-frozen. Total RNA was extracted with TRIzol, reverse-transcribed, and the relative mRNA levels of SIRT1, CREB, and BDNF were determined by the 2^−ΔΔCT method with GAPDH as reference. For protein analysis, hippocampal lysates were resolved by SDS-PAGE and immunoblotted for SIRT1, CREB, p-CREB (Ser133), and BDNF, with β-actin as loading control; band intensities were quantified by grayscale densitometry.

2.8. Statistics

Data are expressed as mean ± SD and analyzed with GraphPad Prism 8.0 and SPSS 23.0. After normality and equal-variance checks, one-way ANOVA with Tukey's post-hoc test was used; non-parametric tests were applied when variances were unequal. Statistical significance was set at $p < 0.05$.

3. Results

3.1. Auricular-Concha EA Reverses Depressive-Like Behavior and Neurological Deficit

Baseline body weight did not differ across groups. By 28 d, PSD rats weighed less than Controls ($p < 0.05$), whereas EA partially restored body weight relative to the model group at 14 d and 28 d ($p < 0.05$; Figure 1A). mNSS rose sharply after MCAO in both model and EA groups versus Control and Sham ($p < 0.05$ at 24 h), and remained elevated in the PSD group. In contrast, mNSS declined progressively in the PSD + EA group and was significantly lower than PSD at 14 d and 28 d ($p < 0.05$; Figure 1B).

In the sucrose-preference, open-field, and forced-swim tests, PSD animals exhibited reduced sucrose preference, fewer crossings and rearings, and longer immobility than Controls ($p < 0.05$; Figure 1C–E). EA significantly increased sucrose preference and locomotion and shortened immobility at 14 d and 28 d relative to PSD ($p < 0.05$). Sham animals remained comparable to Control throughout ($p > 0.05$).

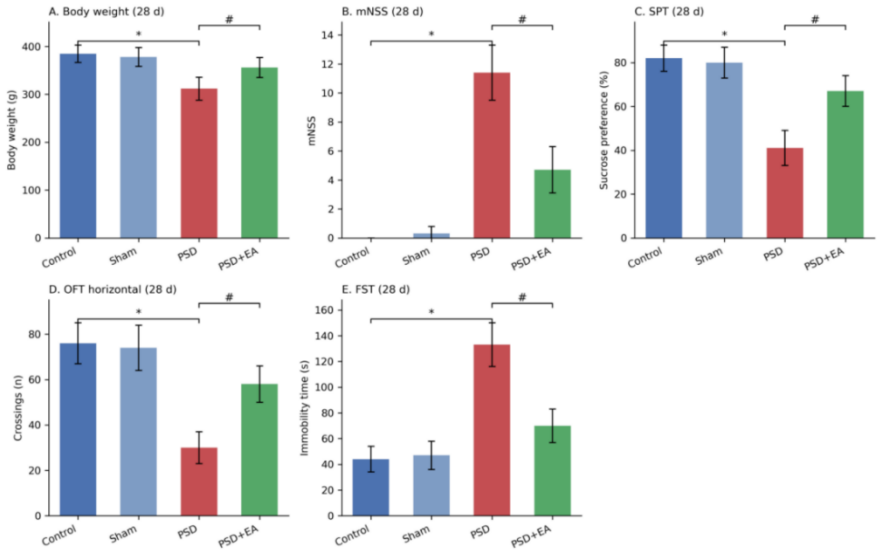

Figure 1. Auricular-concha EA improves behavior and neurological function. (**A**) Body weight; (**B**) mNSS; (**C**) sucrose preference; (**D**) open-field crossing; (**E**) forced-swim immobility. Data are mean ± SD, n = 10. * $p < 0.05$ vs. Control; # $p < 0.05$ vs. PSD.

3.2. Auricular-Concha EA Preserves Hippocampal Neuronal Morphology

HE staining showed that Control and Sham rats had tightly arranged hippocampal neurons with distinct nucleoli and abundant Nissl substance in CA1, CA3, and DG. PSD rats displayed neuronal loss, nuclear pyknosis and hyperchromasia, cytoplasmic vacuolation, and disordered architecture. These histopathological features were markedly attenuated in the PSD + EA group (Figure 2).

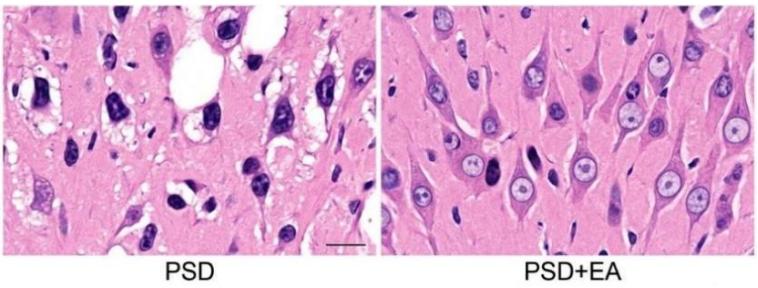

Figure 2. HE staining of hippocampal CA1, CA3, and DG neurons. Representative 40× fields. Scale bar, 50 μm.

3.3. Auricular-Concha EA Increases Hippocampal Cell Proliferation

Immunofluorescence for the proliferation marker Ki67 demonstrated a significant reduction of Ki67-positive cells in CA1, CA3, and DG of PSD rats relative to Control ($p < 0.05$). EA significantly increased Ki67-positive cell numbers in all three subregions compared with PSD ($p < 0.05$; Figure 3). Sham did not differ from Control ($p > 0.05$).

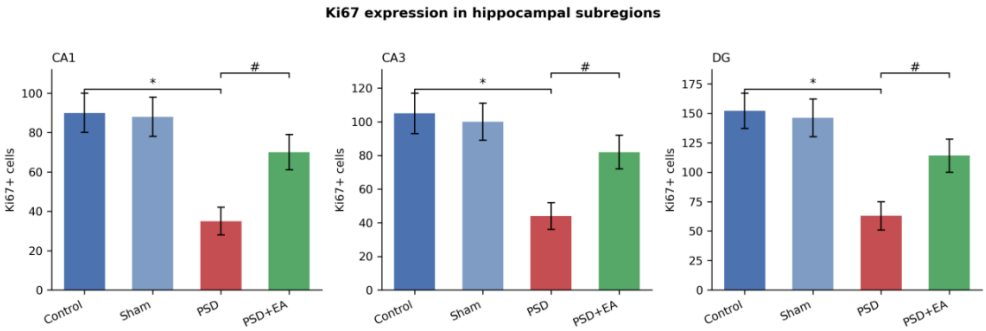

Figure 3. Ki67 immunofluorescence in hippocampal CA1, CA3, and DG. Ki67-positive cells per field. Data are mean ± SD. * $p < 0.05$ vs. Control; # $p < 0.05$ vs. PSD.

3.4. Auricular-Concha EA Upregulates Nestin Expression

Nestin immunoreactivity (% area and positive cell count) was significantly lower in the DG of PSD rats than in Controls ($p < 0.05$). EA significantly elevated Nestin expression above the PSD level ($p < 0.05$), indicative of enhanced progenitor activity and neuronal neogenesis (Figure 4).

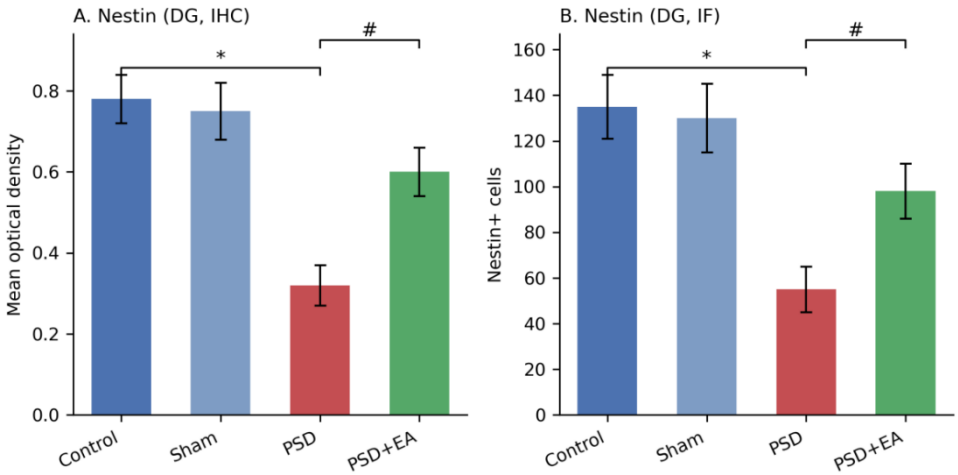

Figure 4. Nestin expression in the hippocampal DG. (**A**) representative immunofluorescence; (**B**) mean optical density. Data are mean ± SD. * $p < 0.05$ vs. Control; # $p < 0.05$ vs. PSD.

3.5. Auricular-Concha EA Restores SIRT1/CREB/BDNF Signaling

RT-PCR revealed significantly reduced mRNA for SIRT1, CREB, and BDNF in PSD hippocampi compared with Control ($p < 0.05$), with EA significantly restoring all three transcripts ($p < 0.05$ vs. PSD; Figure 5). At the protein level, PSD decreased SIRT1, p-CREB, and BDNF without altering total CREB, and EA measurably reversed these reductions ($p < 0.05$ vs. PSD; Figure 5), accompanied by an increased p-CREB/CREB ratio. Sham and Control groups did not differ for any molecular parameter ($p > 0.05$).

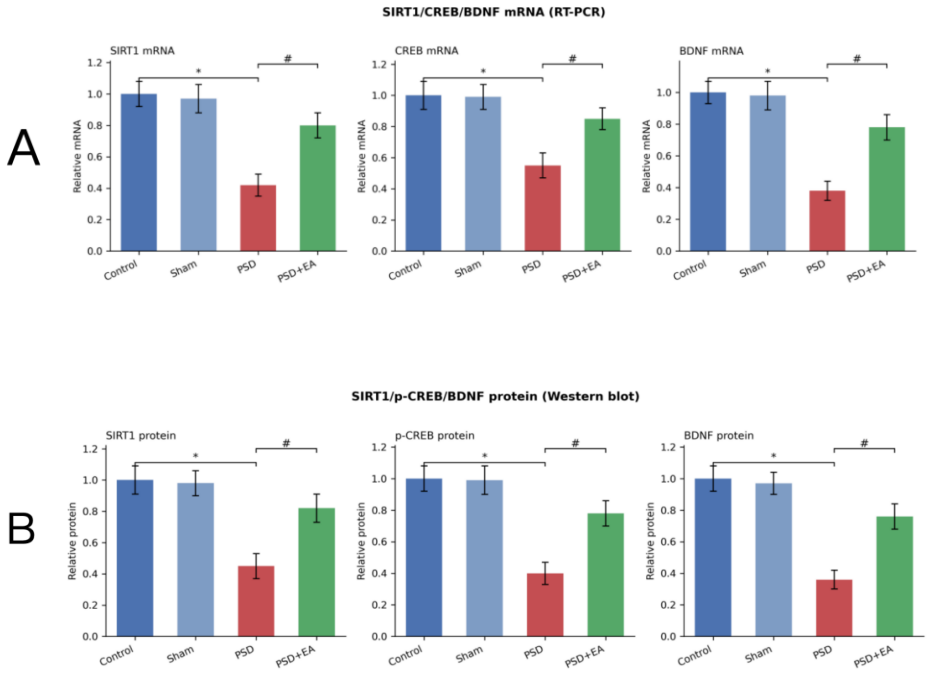

Figure 5. Activation of the SIRT1/CREB/BDNF pathway. (**A**) relative mRNA (RT-PCR); (**B**) representative Western blots and densitometry of SIRT1, p-CREB, and BDNF. Data are mean ± SD. * $p < 0.05$ vs. Control; # $p < 0.05$ vs. PSD.

4. Discussion

The principal finding of this study is that 28 days of auricular-concha EA alleviates depressive-like behavior and neurological impairment in a combined ischemia-plus-stress model of PSD, while simultaneously rescuing hippocampal neurogenesis and re-activating the SIRT1/CREB/BDNF signaling cascade. These results extend prior reports linking auricular vagus nerve stimulation to neuroprotection and antidepressant effects [13,15,16], and provide a specific molecular account for how EA at this site might act in the context of stroke.

Our behavioral results are consistent with the clinical literature showing that acupuncture and EA, alone or as adjuncts to antidepressants, improve mood and daily function in PSD [10–12]. The neurological recovery we observed also echoes our previous demonstration that variable-frequency auricular vagus nerve stimulation reduces infarct size and improves mNSS after ischemia-reperfusion [16]. The concurrent improvement in affect and sensorimotor function suggests a genuine therapeutic effect rather than a nonspecific handling artifact.

The rescue of Ki67-positive cells and Nestin expression indicates that EA reinstates a proliferative, neurogenic state in the hippocampus that is otherwise suppressed in PSD. This is mechanistically important, because impaired neurogenesis is regarded as central to depressive pathophysiology and underlies the delayed onset of antidepressant action [4,5]. The regional pattern—spanning CA1, CA3, and DG—argues against a narrowly localized effect and instead points to a broad trophic response.

At the molecular level, our data implicate the SIRT1/CREB/BDNF axis. PSD downregulated SIRT1, p-CREB, and BDNF while sparing total CREB, and EA restored all three, with a rise in the p-CREB/CREB ratio. This pattern is compatible with SIRT1 acting upstream of CREB phosphorylation and, subsequently, BDNF transcription [6–9]. Notably, exercise and several pharmacological agents have been shown to relieve PSD and depressive-like behavior through SIRT1-dependent BDNF elevation [9,17], and BDNF is consistently reduced in PSD patients [7]. Our findings place auricular-concha EA within this emerging framework, suggesting that vagal afferent recruitment at the concha engages the same neurotrophic program through SIRT1/CREB/BDNF.

Several caveats temper interpretation. First, we did not perform loss-of-function manipulations to prove causality of the SIRT1/CREB/BDNF pathway; inhibiting SIRT1 or CREB would be required to establish directionality. Second, neurogenesis was evaluated using Ki67 and Nestin, which mark proliferation and progenitors but do not demonstrate maturation or functional integration of new neurons; double labeling with BrdU/NeuN is needed in future work. Third, only a single stimulation parameter set was tested, precluding conclusions about optimal frequency or duration. Fourth, alternative mechanisms—including neuroinflammation and hypothalamic-pituitary-adrenal regulation—were not systematically profiled here, although our group has reported anti-inflammatory actions of auricular vagus nerve stimulation elsewhere [16].

In conclusion, auricular-concha EA attenuates depressive-like behavior and neurological deficit and promotes hippocampal neurogenesis in PSD rats, in association with activation of the SIRT1/CREB/BDNF pathway. These data rationalize further translational and dose-ranging studies aimed at positioning auricular-concha EA as an adjunct treatment for post-stroke depression.

Funding

This work was supported by the Guangdong Provincial Administration of Traditional Chinese Medicine General Project (Grant No. 20251374).

Author Contributions

Writing—original draft, T.C., Y.Z., J.H. and G.Z.; writing—review and editing, T.C., Y.Z., J.H. and G.Z. All authors have read and agreed to the published version of the manuscript.

Institutional Review Board Statement

Not applicable.

Informed Consent Statement

Not applicable.

Data Availability Statement

Not applicable.

Conflicts of Interest

The authors declare no conflict of interest.

References

1. Guo J, Wang J, Sun W, *et al.* The Advances of Post-Stroke Depression: 2021 Update. *Journal of Neurology* 2022; **269**(**3**): 1236–1249. https://doi.org/10.1007/s00415-021-10597-4.
2. Liu L, Zhang G, He Y, *et al.* Post-Stroke Depression and Its Impact on Mortality and Functional Outcomes: A Systematic Review and Meta-Analysis. *NeuroRehabilitation* 2026. https://doi.org/10.1177/10538135261462562.
3. Mușat MI, Cătălin B, Hadjiargyrou M, *et al.* Advancing Post-Stroke Depression Research: Insights from Murine Models and Behavioral Analyses. *Life* 2024; **14**(**9**): 1110. https://doi.org/10.3390/life14091110.
4. Peng MS, Jiang J, Polizzi L, *et al.* Dysregulated Adult Hippocampal Neurogenesis in Major Depressive Disorder. *Nature Medicine* 2026. https://doi.org/10.1038/s41591-026-04571-8.
5. Farooqui SA, Santerre M, Shcherbik N, *et al.* Memory Impairments: Type, Causes, and Molecular Players—Memory Dysfunction across Neurologic Insults. *Cells* 2026; **15**(**10**): 923. https://doi.org/10.3390/cells15100923.
6. Li LP, Tong HHY. Cocoa Polyphenols in Brain Health: BDNF/CREB-Mediated Mechanisms in Depression, Cognition, and the Gut–Brain Axis. *Frontiers in Nutrition* 2026; **13**: 1859145. https://doi.org/10.3389/fnut.2026.1859145.
7. Shi T, Wang X, Zhou H. Brain-Derived Neurotrophic Factor as a Predictor of Post-Stroke Depression: An Updated Systematic Review and Meta-Analysis. *Neuropsychological Rehabilitation* 2026. https://doi.org/10.1080/09602011.2026.2658483.
8. Qiu X, Lu P, Zeng X, *et al.* Study on the Mechanism for SIRT1 during the Process of Exercise Improving Depression. *Brain Sciences* 2023; **13**(**5**): 719. https://doi.org/10.3390/brainsci13050719.
9. Tang J, Lu L, Yuan J, *et al.* Exercise-Induced Activation of SIRT1/BDNF/mTORC1 Signaling Pathway: A Novel Mechanism to Reduce Neuroinflammation and Improve Post-Stroke Depression. *Actas Españolas de Psiquiatría* 2025; **53**(**2**): 366. https://doi.org/10.62641/aep.v53i2.1838.
10. Lam Ching W, Li HJ, Guo J, *et al.* Acupuncture for Post-Stroke Depression: A Systematic Review and Network Meta-Analysis. *BMC Psychiatry* 2023; **23**(**1**): 314. https://doi.org/10.1186/s12888-023-04749-1.
11. Liu R, Zhang K, Tong Q, *et al.* Acupuncture for Post-Stroke Depression: A Systematic Review and Meta-Analysis. *BMC Complementary Medicine and Therapies* 2021; **21**(**1**): 109. https://doi.org/10.1186/s12906-021-03277-3.
12. Zhang Z, Xue K, Li H, *et al.* Electroacupuncture for Post-Stroke Depression: A Systematic Review and Meta-Analysis of Randomized Controlled Trials. *Frontiers in Neurology* 2025; **16**: 1671808 https://doi.org/10.3389/fneur.2025.1671808.
13. Shi A, Li W, Liu X, *et al.* Acupuncture for Depression: Decoding Neuroimmune Crosstalk and Targeting Anti-Inflammatory Mechanisms. *Current Opinion in Pharmacology* 2025. https://doi.org/10.1016/j.coph.2025.102585.
14. Yang J, Jia N. Advances of Research on Auricular Vagus Nerve Stimulation for Treatment of Nervous System Diseases. *Journal of Biosciences and Medicines* 2023; **11**(**4**): 1–14.
15. Yang Q, Zhou Y, Tang H, *et al.* Transcutaneous Auricular Vagus Nerve Stimulation Attenuates Depressive-Like Behaviors Via Enhancing Neuroplasticity and Regulating the ALK5/Smad2/3/Gadd45β Signaling Pathway in Rats with Post-Stroke Depression. *Frontiers in Immunology* 2026; 17: 1755707. https://doi.org/10.3389/fimmu.2026.1755707.
16. Yang J, Jia N, Ou Z, *et al.* The Alleviation of Variable-Frequency aVNS on Neuroinflammatory Injury in Ischemia-Reperfusion Rats Is Related to the Inhibition of TLR4 Expression. *Minerva Medica* 2024; **115**(**2**): 214-215. https://doi.org/10.23736/S0026-4806.23.08638-X.
17. Liu Y, Li Y, Li J, *et al.* Gypenosides Alleviate Oxidative Stress in the Hippocampus, Promote Mitophagy, and Mitigate Depressive-Like Behaviors Induced by CUMS Via SIRT1. *Journal of Ethnopharmacology* 2025. https://doi.org/10.1016/j.jep.2024.118823.